Hindawi
International Journal of Photoenergy
Volume 2020, Article ID 3082835, 8 pages
https://doi.org/10.1155/2020/3082835

Research Article

Annealing Effects on GaAs/Ge Solar Cell after 150 keV Proton Irradiation

Meihua Fang,[1] **Tao Fei**,[1] **Mengying Bai**,[1] **Yipan Guo**,[1] **Jingpeng Lv**,[1] **Ronghui Quan**,[1] **Hongbo Lu**,[2] **and Huiping Liu**[3]

[1]*Nanjing University of Aeronautics and Astronautics, Nanjing 210016, China*
[2]*State Key Laboratory of Space Power-Sources, Shanghai Institute of Space Power-Sources, Shanghai 200245, China*
[3]*Institute of Modern Physics, Chinese Academy of Sciences, Lanzhou, Gansu 730000, China*

Correspondence should be addressed to Meihua Fang; fmh_medphys@nuaa.edu.cn

Received 26 August 2019; Revised 18 December 2019; Accepted 23 January 2020; Published 26 February 2020

Academic Editor: Leonardo Sandrolini

Radiation-induced defects are responsible for solar cell degradation. The effects of radiation and annealing on the defects of a GaAs/Ge solar cell are modeled and analyzed in this paper. The electrical performance and spectral response of solar cells irradiated with 150 keV proton are examined. Then, thermal annealing was carried out at 120°C. We found that the proportion of defect recovery after annealing decreases with increasing irradiation fluence. The minority carrier lifetime increases with decreasing defect concentration, which means that the electrical performance of the solar cell is improved. We calculated the defect concentration and minority carrier lifetime with numerical simulation and modeled an improved annealing kinetic equation with experimental results.

1. Introduction

Space radiation produced damage in solar cells, which will limit the capability and lifetime of satellites. In order to mitigate the space radiation damage, the mechanisms of radiation-induced degradation of the solar cell have been heavily studied [1–5]. It is clear that interactions between energetic particles and nucleus result displacement damage and induce lattice defects in materials. Defects act as recombination centers in the band gap and have a significant impact on the minority carrier lifetime, a parameter that determines the electric performance of solar cells [6–14].

The minority carrier lifetime for solar cells is extremely sensitive to defects and increases with the decrease of defect concentration [15–17]. Defects in semiconductor material can be recovered via thermal annealing. There are two ways to anneal cell damage, postirradiation annealing and continuous annealing. Continuous annealing means that solar cells are radiated at a high temperature that the defects are produced by irradiation and recovered by thermal annealing simultaneously. Some results show that continuous annealing could reduce the concentration of defects above a certain temperature [13, 18]. In earth orbit, the solar array will be heated to above 100°C [19, 20], and the recovery of radiation defects will be more rapid with the high temperature. Therefore, it is necessary to consider the effect of temperature on radiation defects when studying the radiation degradation of solar cells.

In this paper, single-junction GaAs/Ge solar cells were irradiated with 150 keV proton, and the irradiated solar cells were annealed at 120°C. Then, we used an improved defect annealing kinetic equation to calculate the defect concentration. And based on the defect concentration, the simulation of short-circuit current during the annealing process was in good agreement with the experimental results.

2. Experimental

The samples used in this work are GaAs/Ge single-junction solar cells manufactured by metal organic chemical vapor deposition (MOCVD). The cell size is $10 \times 10\,\text{mm}^2$, and the structure is shown in Figure 1. The samples were irradiated

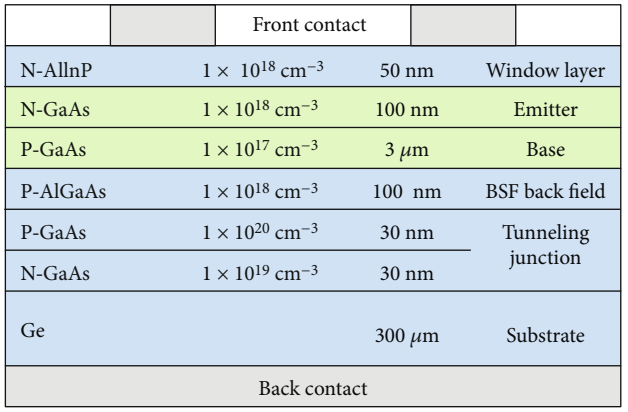

Figure 1: Schematic diagrams of GaAs/Ge cells used in the study.

Table 1: The fluence setting in irradiation experiment.

Group	Fluence (cm^{-2})
1	1×10^{10}
2	5×10^{10}
3	1×10^{11}
4	5×10^{11}
5	0

with 150 keV proton under vacuum at room temperature, and the irradiation fluence is listed in Table 1. The irradiation experiments were carried out in the State Key Laboratory of Space Environmental Material Behavior and Evaluation Technology, Harbin Institute of Technology.

I-V characteristics and spectral response (also called external quantum efficiency (EQE)) were measured under AM0 conditions (0.1367 W/cm^2) at 25°C. The cell surface reflectance was measured simultaneously with EQE on a Quantum Efficiency Tester (model: Enlitech QE-R). Thermal annealing was carried out at 120°C, and meanwhile, the short-circuit current was measured every ten minutes in situ.

3. Results and Discussion

3.1. Degradation Behaviors of Electrical Properties. The *I-V* characteristics of the GaAs/Ge solar cell irradiated with various fluence were shown in Figure 2. Clearly, the performance of the solar cell was declined with increasing irradiation fluence. The normalized degradation of I_{SC}, V_{OC}, and P_{max}

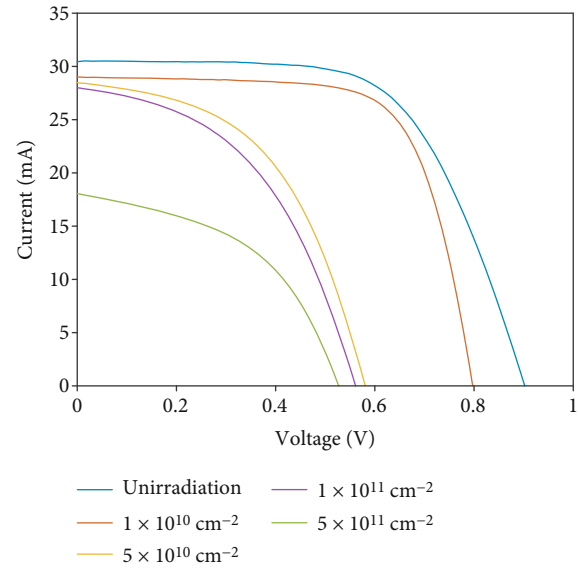

Figure 2: The *I-V* characteristics of the GaAs/Ge solar cell irradiated by 150 keV proton.

versus fluence was shown in Figure 3(a). It can be seen from Figure 3(a) that when fluence is smaller than 1×10^{11} cm^{-2}, the degradation of V_{OC} is more serious than that of I_{SC}. When fluence increases to 5*e*11 cm^{-2}, I_{SC} decreased quickly while V_{OC} is almost unchanged. This unusual decrease of I_{SC} can be explained by the degradation of EQE with fluence which is shown in Figure 3(b). EQE in short wavelength ($\lambda < 650$ nm) declined more severe than that in long wavelength ($\lambda > 650$ nm) when the irradiated fluence is 5*e*11 cm^{-2}.

3.2. Simulation of I_{SC} Degradation Behaviors. The steady-state operating characteristics of solar cells can be described by the minority carrier diffusion equations [21]

$$\begin{cases} D_p \dfrac{d^2 \Delta p_n}{dx^2} - \dfrac{\Delta p_n}{\tau_p} = -G(x), \\ D_n \dfrac{d^2 \Delta n_p}{dx^2} - \dfrac{\Delta n_p}{\tau_n} = -G(x). \end{cases} \quad (1)$$

The meaning of all parameters is shown in Table 2.

The current density of emitter, base, and space charge regions can be deduced from the above minority carrier diffusion equations [21, 22]:

$$\begin{cases} J_e = \dfrac{qF(1-R)\alpha L_e}{\alpha^2 {L_e}^2 - 1} \left[\dfrac{s_e + \alpha L_e - (s_e \cosh(w_e/L_e) + \sinh(w_e/L_e)) \exp(-\alpha w_e)}{s_e \sinh(w_e/L_e) + \cosh(w_e/L_e)} - \alpha L_e \exp(-\alpha w_e) \right], \\ J_b = \dfrac{qF(1-R)\alpha L_b}{\alpha^2 {L_b}^2 - 1} \left[\alpha L_b - \dfrac{s_b \cosh(w_b/L_b) + \sinh(w_b/L_b) + (\alpha L_b - s_b) \exp(-\alpha w_b)}{s_b \sinh(w_b/L_b) + \cosh(w_b/L_b)} \right], \\ J_{scr} = qF(1-R) \exp(-\alpha w_e)[1 - \exp(-\alpha w_{scr})]. \end{cases} \quad (2)$$

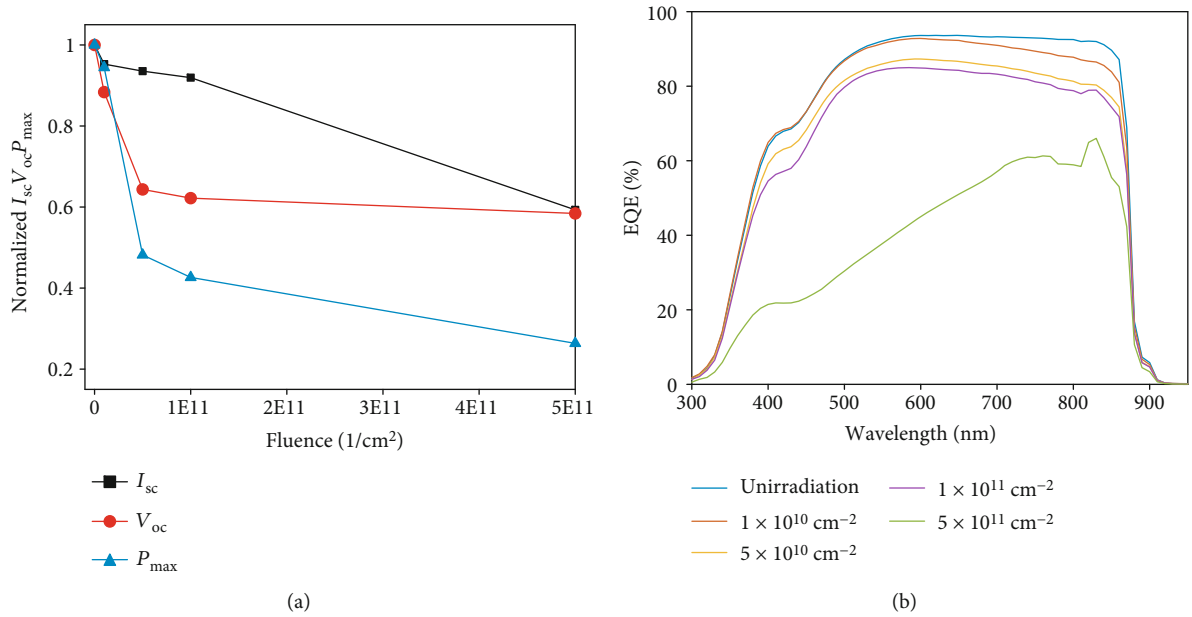

Figure 3: The electric performance and EQE for GaAs solar cells irradiated with 150 keV proton: (a) degradation of I_{SC}, V_{OC}, and P_{max}; (b) EQE.

Table 2: Parameters in the minority carrier diffusion equations (Equation (1)).

Parameters	Description
D_p	Hole diffusion coefficient
D_n	Electron diffusion coefficient
Δp_n	Hole concentration in the n-type material
Δn_p	Electron concentration in the p-type material
τ_p	Minority carrier hole lifetimes
τ_n	Minority carrier electron lifetimes
x	Depth from the front surface of the solar cell
$G(x)$	Optical generation rate of electron-hole pairs

The meaning and value of parameters in the above formula are shown in Table 3. Among them, minority carrier diffusion length L_e/L_b and simplified surface recombination rate s_e/s_b are related to the minority carrier lifetime, which means that these parameters will change with the minority carrier lifetime. In addition, some parameters related to wavelength are shown as a graph, in which F is the photon flux incident cell surface and $F(\lambda) = \phi(\lambda) \cdot \lambda/hc$. In this equation, $\phi(\lambda)$ is an air mass zero reference spectrum developed by the American Society for Testing and Materials [23]. α is the photon absorption rate of GaAs; here, what we used was the experimental value published by Aspnes et al. [24]. R is surface reflectivity of the solar cell. These wavelength-dependent parameters are shown in Figures 4 and 5.

The short-circuit current density J_{sc} is the sum of contributions from each of the three regions listed in Equation (2), which can be expressed as

$$\begin{cases} J(\lambda) = J_e(\lambda) + J_b(\lambda) + J_{scr}(\lambda), \\ J = \int_0^{Eg} J(\lambda) d\lambda, \end{cases} \tag{3}$$

where Eg is bandgap, for GaAs is 1.424 eV, corresponding to the wavelength of 871 nm.

According to Equations (2) and (3), J_{sc} is a function of minority carrier lifetime τ, a parameter commonly used to evaluate solar cell performance. An effective minority carrier lifetime is given as

$$\frac{1}{\tau} = \frac{1}{\tau_r} + \frac{1}{\tau_{nr}} + \frac{1}{\tau_{Auger}}, \tag{4}$$

where τ_r, τ_{nr}, and τ_{Auger} represent the minority carrier lifetime of radiative, nonradiative (SRH reorganization), and Auger recombination, respectively. For unirradiated GaAs solar cells, τ_r is about 40 ns, τ_{nr} is 870 ns [25], and τ_{Auger} is usually ignored for its effect is much smaller than that of the other two recombination mechanisms. The nonradiative recombination minority carrier lifetime decreases with increasing defect concentration:

$$\frac{1}{\tau_{nr}} = \frac{1}{\tau_{nr\_0}} + N\sigma v_{th}, \tag{5}$$

where σ is defect capture cross-section with a value of 4×10^{-13} cm^2, v_{th} is thermal velocity of the carriers with

Table 3: Parameters in the current density equation (Equation (2)) are derived from the minority carrier diffusion equation.

Parameters	Description	Value
q	Quantity of electric charge	1.602×10^{-19} C
w_e	Emitter thickness	0.1 μm
w_b	Base thickness	2.97 μm
w_{scr}	Space charge zone thickness	0.03 μm
D_e	Emission zone minority carrier diffusion coefficient	6.63 cm^2/s
D_b	Base zone minority carrier diffusion coefficient	1.93 cm^2/s
S_e	Front surface recombination rate	1×10^4 cm/s
S_b	Back surface recombination rate	4×10^4 cm/s
τ	Minority carrier lifetime	38 ns
L_e	Emission zone minority carrier diffusion length, $L_e = \sqrt{D_e \tau}$	4.17 μm
L_b	Base zone minority carrier diffusion length, $L_b = \sqrt{D_b \tau}$	7.72 μm
s_e	Simplified front surface recombination rate, $s_e = S_e L_e / D_e$	2.16
s_b	Simplified back surface recombination rate, $s_b = S_b L_b / D_b$	4.66

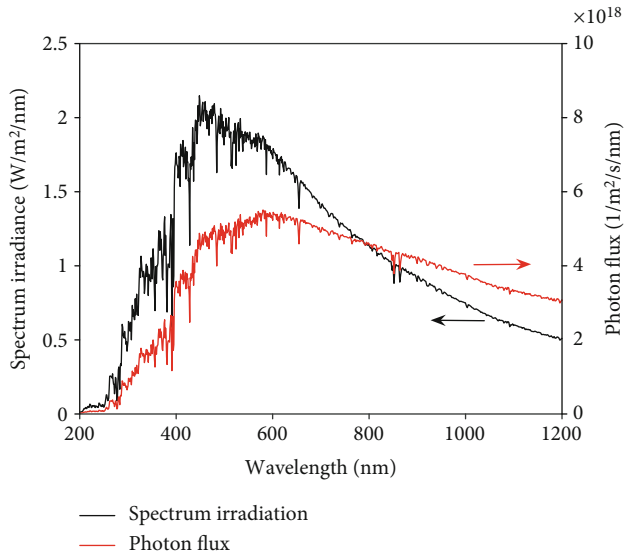

Figure 4: The AM0 solar spectrum irradiance and corresponding photon flux.

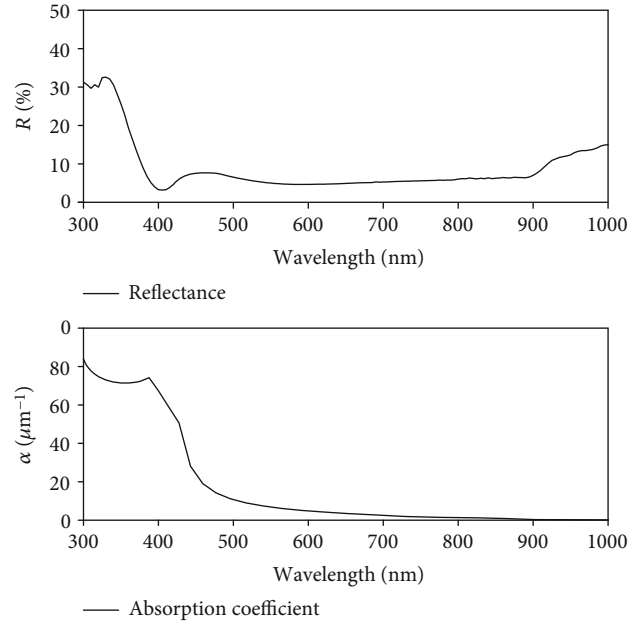

Figure 5: The photon absorption coefficient of GaAs and front surface reflectance of the solar cell before irradiation.

a value of 4.4×10^7 cm/s [6], and N is the concentration of defects, $N = k\varphi$ and $k = \beta E_{niel}$, in which φ is fluence, k is the introduction rate (the number of defects induced by the incident particle), β is a constant coefficient and its value is 3.76×10^3 g/MeV/cm^3 [11, 26], and E_{niel} (nonionizing energy loss) for 150 keV proton is 0.259 MeV·cm^2/g [27], so k of 150 keV proton is 974 cm^{-1}. In fact, irradiation will produce a series of defects with different defect energy levels in the forbidden band, in which deep defect energy levels can function as significant recombination centers. Here, k refers to the introduction rate of these defects, whose energy levels are near Ev+0.71 and Ec-0.71. Thus, the effective minority carrier lifetime can be expressed as

$$\frac{1}{\tau} = \frac{1}{\tau_r} + \frac{1}{\tau_{nr}} + k\varphi\sigma v_{th}. \quad (6)$$

We calculated the defect concentration and minority carrier lifetime with 150 keV proton fluence (seen in Figure 6) by Equation (6). Here, the introduction rate is a constant; that is,

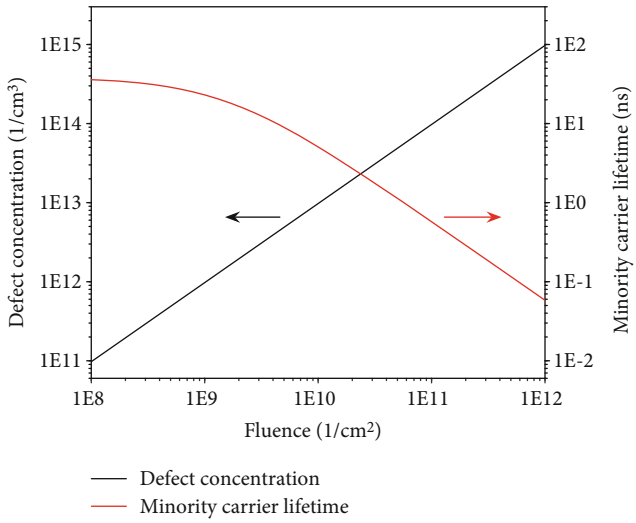

Figure 6: The defect concentration and minority carrier lifetime vs. 150 keV proton fluence.

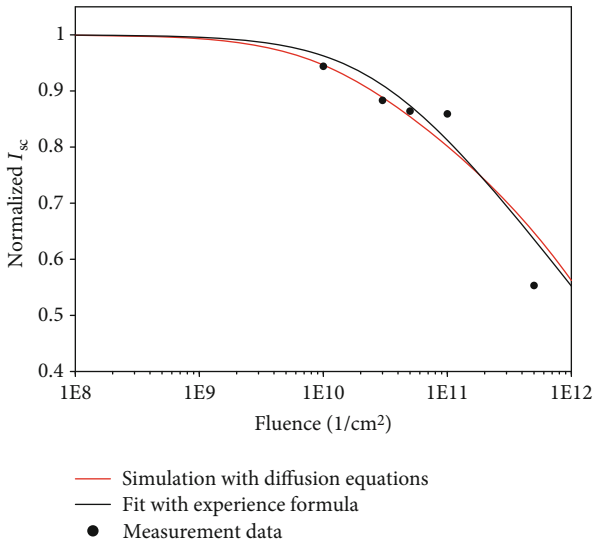

Figure 7: The normalized I_{SC} vs. 150 keV proton fluence. The red curve is the result of calculation, and the black curve is the fitting result of experimental data.

there is no correlation between two independent incidents. So, the defects are increasing linearly with irradiation fluence, and the minority carrier lifetime is also decreasing continuously.

To verify the accuracy and parameter settings of Equation (2), we substitute the correspondence between minority carrier lifetime and fluence into Equation (2); the result is shown in Figure 7. In addition, the normalized I_{SC} vs. fluence fitted with $I/I_0 = 1 - A \times \log(1 + \varphi/\varphi_0)$ is also shown in Figure 7, where the fitting parameter A is 0.2879 and φ_0 is 2.8663×10^{10} cm^{-2}. Mean square error of fitting results and numerical calculation results compared with the experimental data, respectively, are 25% and 19%.

3.3. Thermal Annealing. Studies show that after thermal annealing, the irradiation damage of solar cells will be partially recovered [18, 28]. Figure 8 shows that the normalized I_{SC} increases at an annealing temperature of 120°C. The normalized factor in this figure is I_{SC} before irradiation at 120°C, for the short-circuit current will increase with temperature [29, 30]. The fact that I_{SC} increases with annealing time indicates that the radiation damage is recovered by thermal annealing.

The annealing kinetics of radiation defects can be expressed as [7, 31]

$$\frac{dN}{dt} = -\alpha N, \tag{7}$$

where t is annealing time, α is the annealing rate, and dN/dt is the annealing efficiency. Obviously dN/dt is decreasing with the defect concentration. N can be obtained by integrating Equation (7) [7]:

$$N = N_0 \exp(-\alpha t), \tag{8}$$

where N_0 is the initial defect concentration before annealing. According to Equation (8), defect concentration will decrease continuously until all defects are recovered. That is to say, the defects related in Equation (8) are all recoverable radiation defects. However, experiments show that some radiation defects are stable at the annealing temperature and the defects are partially recovered after thermal annealing [7, 9, 18, 32]. Accordingly, the radiation-induced defects can be divided into two types; that is, defects can be or cannot be recovered by annealing. Based on this fact, Equation (8) can be rewritten as

$$N = (1 - p)N_0 \exp(-\alpha t) + pN_0, \tag{9}$$

where p is the proportion of defects cannot be recovered.

Figure 8 shows the fitted results with I_{SC} and Equation (9). The annealing rate α, proportion of stable defects p, defect concentration, and minority carrier lifetime before and after annealing are shown in Table 4. The annealing rate α is 5.167×10^{-4} s^{-1} in this annealing condition. As shown in Figure 9, p increases with irradiation fluence and increases quickly at lower irradiation fluences, then becomes saturated at higher irradiation fluences. This means that the higher the irradiation fluence, the smaller the proportion of defects that can be recovered after annealing. That is because point defects tend to cluster with increasing irradiation fluence and clustered defects are more difficult to be recovered. The defect concentration after annealing is decreased dramatically compared to the defects before annealing. Based on the defect concentration and Equation (5), the minority carrier lifetime before and after annealing can be calculated as listed in Table 4. It is clear that the minority carrier lifetime after annealing increases and the defect concentration decreases.

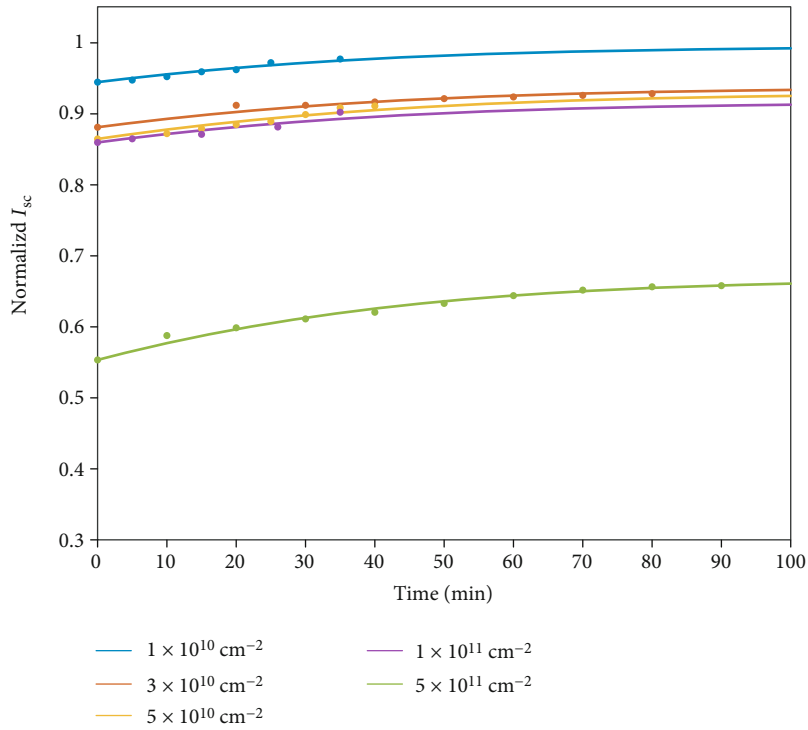

Figure 8: In situ measurement for I_{SC} during annealing and corresponding fitting results.

Table 4: The defect concentration and minority carrier lifetime before and after annealing and the annealing rate and the proportion of irrecoverable defects.

Fluence (1/cm^2)	N (1/cm^3)		τ (ns)		α (1/s)	p (%)
	Before annealing	After annealing	Before annealing	After annealing		
1×10^{10}	1.19×10^{13}	2.48×10^{12}	4.49	17.45		6.30
3×10^{10}	3.92×10^{13}	1.80×10^{13}	1.42	3.02		35.94
5×10^{10}	5.03×10^{13}	2.19×10^{13}	1.11	2.50	5.167×10^{-4}	33.22
1×10^{11}	5.39×10^{13}	2.67×10^{13}	1.04	2.07		40.17
5×10^{11}	9.02×10^{14}	4.88×10^{14}	0.06	0.12		45.58

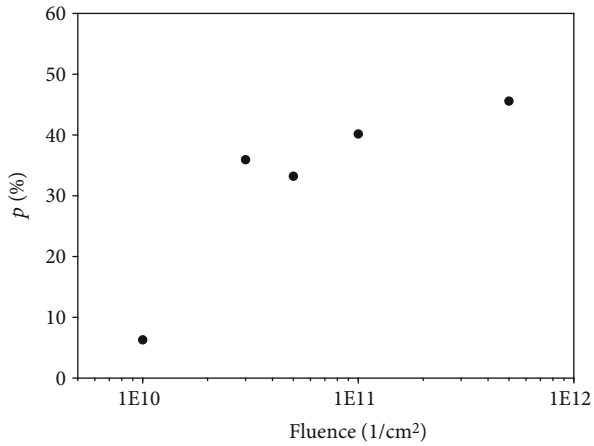

Figure 9: p increases with irradiation fluence increase.

4. Conclusion

The degradation of GaAs solar cells in electrical properties can be enhanced by increasing the proton fluence. However, it can be improved in the process of thermal annealing. The short-circuit current after irradiation and annealing can be studied by the minority diffusion equation. Based on the experiment results and theoretical analysis, an improved annealing kinetic equation is carried out. I_{SC} calculated by the minority diffusion equation and the improved annealing formula agrees well with the experimental results. From our analyzation, the defects can be partially recovered after annealing. Furthermore, the proportion of stable defects is the defects unrecovered after annealing increases with increasing irradiation fluence for the reason of clustered defects. The minority carrier lifetime increases dramatically in this annealing experiment.

Data Availability

The data used to support the findings of this study are included within the article.

Additional Points

Highlights. (i) Defect concentration and minority carrier lifetime are modeled and analyzed after irradiation and during thermal annealing. (ii) The annealing kinetic equation is developed to describe the defect change.

Conflicts of Interest

The authors declare that they have no conflicts of interest.

Acknowledgments

This work was supported by the Shanghai Institute of Space Power-Sources, and the solar cells used in the experiment were also provided by it. The work was funded by the Fundamental Research Funds for the Central Universities, No. NS2019052.

References

[1] M. Levalois, P. Bogdanski, and M. Toulemonde, "Induced damage by high energy heavy ion irradiation at the GANIL accelerator in semiconductor materials," *Nuclear Instruments and Methods in Physics Research Section B: Beam Interactions with Materials and Atoms*, vol. 63, no. 1-2, pp. 14–20, 1992.

[2] W. Rong, G. Zengliang, Z. Xinghui, and Z. Zuoxu, "5-20 MeV proton irradiation effects on GaAs/Ge solar cells for space use," *Solar Energy Materials and Solar Cells*, vol. 77, no. 4, pp. 351–357, 2003.

[3] H. Jianmin, W. Yiyong, X. Jingdong, Y. Dezhuang, and Z. Zhongwei, "Degradation behaviors of electrical properties of GaInP/GaAs/Ge solar cells under <200keV proton irradiation," *Solar Energy Materials and Solar Cells*, vol. 92, no. 12, pp. 1652–1656, 2008.

[4] M. Ochoa, E. Yaccuzzi, P. Espinet-González et al., "10 MeV proton irradiation effects on GaInP/GaAs/Ge concentrator solar cells and their component subcells," *Solar Energy Materials and Solar Cells*, vol. 159, pp. 576–582, 2017.

[5] M. Imaizumi, T. Nakamura, T. Takamoto, T. Ohshima, and M. Tajima, "Radiation degradation characteristics of component subcells in inverted metamorphic triple-junction solar cells irradiated with electrons and protons," *Progress in Photovoltaics: Research and Applications*, vol. 25, no. 2, pp. 161–174, 2017.

[6] S. S. Li and R. Y. Loo, "Deep-level defects and numerical simulation of radiation damage in GaAs solar cells," *Solar Cells*, vol. 31, no. 4, pp. 349–377, 1991.

[7] S. A. Goodman, F. D. Auret, and G. Myburg, "Defect annealing of alpha-particle irradiated n-GaAs," *Applied Physics A*, vol. 59, no. 3, pp. 305–310, 1994.

[8] P. J. Hautojärvi, "Defects in semiconductors: recent progress in positron experiments," *Materials Science Forum*, vol. 175-178, pp. 47–58, 1994.

[9] D. Stievenard, X. Boddaert, and J. C. Bourgoin, "Irradiation-induced defects inp-type GaAs," *Physical Review B*, vol. 34, no. 6, pp. 4048–4058, 1986.

[10] J. H. Warner, S. R. Messenger, R. J. Walters, S. A. Ringel, and M. R. Brenner, "A deep level transient spectroscopy study of electron and proton irradiated p^+n GaAs diodes," in *2009 European Conference on Radiation and Its Effects on Components and Systems*, Bruges, Belgium, 2009.

[11] L. Ming, W. Rong, Y. Kui, and Y. Tiancheng, "Photoluminescence analysis of electron irradiation-induced defects in GaAs/Ge space solar cells," *Nuclear Instruments and Methods in Physics Research Section B: Beam Interactions with Materials and Atoms*, vol. 312, pp. 137–140, 2013.

[12] J.-L. Wang, T.-C. Yi, Y. Zheng, R. Wu, and R. Wang, "Temperature-dependent photoluminescence analysis of 1.0 MeV electron irradiation-induced nonradiative recombination centers in n^+-p GaAs middle cell of GaInP/GaAs/Ge triple-junction solar cells," *Chinese Physics Letters*, vol. 34, no. 7, article 076106, 2017.

[13] J. H. Heinbockel, E. J. Conway, and G. H. Walker, "Simultaneous radiation damage and annealing of GaAs solar cells," in *Proceedings of the 14th IEEE Photovoltaic Specialists Conference*, pp. 1085–1089, San Diego, CA, USA, 1980.

[14] Y. Yan, M. Fang, X. Tang et al., "Effect of 150 keV proton irradiation on the performance of GaAs solar cells," *Nuclear Instruments and Methods in Physics Research Section B: Beam Interactions with Materials and Atoms*, vol. 451, pp. 49–54, 2019.

[15] L. Ji, M. Tan, C. Ding et al., "The striking influence of rapid thermal annealing on InGaAsP grown by MBE: material and photovoltaic device," *Journal of Crystal Growth*, vol. 458, pp. 110–114, 2017.

[16] M. Xiao, G. Chen, R. Yang et al., "Effect of high temperature rapid thermal annealing on optical properties of InGaAsP grown by molecular beam epitaxy," *Optical Materials Express*, vol. 7, no. 11, pp. 3826–3835, 2017.

[17] T. Sasaki, K. Arafune, H. S. Lee et al., "Effects of thermal cycle annealing on reduction of defect density in lattice- mismatched InGaAs solar cells," *Physica B: Condensed Matter*, vol. 376-377, pp. 626–629, 2006.

[18] R. Y. Loo, G. S. Kamath, and S. S. Li, "Radiation damage and annealing in GaAs solar cells," *IEEE Transactions on Electron Devices*, vol. 37, no. 2, pp. 485–497, 1990.

[19] E. Azadi, S. Ahmad Fazelzadeh, and M. Azadi, "Thermally induced vibrations of smart solar panel in a low-orbit satellite," *Advances in Space Research*, vol. 59, no. 6, pp. 1502–1513, 2017.

[20] J. Li and S. Yan, "Thermally induced vibration of composite solar array with honeycomb panels in low earth orbit," *Applied Thermal Engineering*, vol. 71, no. 1, pp. 419–432, 2014.

[21] A. Luque and S. Hegedus, *Handbook of Photovoltaic Science and Engineering*, John Wiley & Sons, Ltd, 2003.

[22] W. J. Yang, Z. Q. Ma, X. Tang, C. B. Feng, W. G. Zhao, and P. P. Shi, "Internal quantum efficiency for solar cells," *Solar Energy*, vol. 82, no. 2, pp. 106–110, 2008.

[23] M. Taylor, "IKONOS Planetary Reflectance and Mean Solar Exoatmospheric Irradiance. ASTM Standard Extraterrestrial Spectrum Reference," 2005, https://www.nrel.gov/grid/solar-resource/spectra-astm-e490.html.

[24] D. E. Aspnes, S. M. Kelso, R. A. Logan, and R. Bhat, "Optical properties of $Al_xGa_{1-x}As$," *Journal of Applied Physics*, vol. 60, no. 2, pp. 754–767, 1986.

[25] E. E. Perl, D. Kuciauskas, J. Simon, D. J. Friedman, and M. A. Steiner, "Identification of the limiting factors for high-temperature GaAs, GaInP, and AlGaInP solar cells from device and carrier lifetime analysis," *Journal of Applied Physics*, vol. 122, no. 23, article 233102, 2017.

[26] S. Makham, M. Zazoui, G. C. Sun, and J. C. Bourgoin, "Prediction of proton-induced degradation of GaAs space solar cells," *Solar Energy Materials and Solar Cells*, vol. 90, no. 10, pp. 1513–1518, 2006.

[27] "Screened Relativistic (SR) Nuclear Stopping Power Calculator (version 6.0.1)," http://www.sr-niel.org/index.php/sr-niel-web-calculators/niel-calculator-for-electrons-protons-and-ions.

[28] M. Yamaguchi and K. Ando, "Mechanism for radiation resistance of InP solar cells," *Journal of Applied Physics*, vol. 63, no. 11, pp. 5555–5562, 1988.

[29] J. C. C. Fan, "Theoretical temperature dependence of solar cell parameters," *Solar Cells*, vol. 17, no. 2-3, pp. 309–315, 1986.

[30] M. Abderrezek, M. Fathi, S. Mekhilef, and F. Djahli, "Effect of temperature on the GaInP/GaAs tandem solar cell performances," *International Journal of Renewable Energy Research*, vol. 5, pp. 629–634, 2015.

[31] J. Bourgoin and M. Lannoo, *Point Defects in Semiconductors II*, Springer, Berlin, Heidelberg, 1983.

[32] R. J. Walters and G. P. Summers, "Deep level transient spectroscopy study of proton irradiatedp-type InP," *Journal of Applied Physics*, vol. 69, no. 9, pp. 6488–6494, 1991.